

# An Exploration of Information-Theoretic Measures in the Computational Dynamics of Cellular Automata

Warren D. Craft

Department of Computer Science  
The University of New Mexico  
Albuquerque, NM, USA  
wdcraft@unm.edu

**Abstract**—Information-theoretic measures (such as entropy ( $H$ ), transfer entropy (TE), mutual information (MI), and local active information storage (LAIS)) were used to analyze the computational dynamics of cellular automata (CAs) applied to a majority density-classification task, and the CAs were used to help understand commonly-used information-theoretic measures. Some unexpected relationship(s) were discovered among  $H$ , TE, and MI, and preliminary results for local information-theoretic measures make clear that complicated and nuanced interpretations are required and suggest that local information-theoretic measures will be highly sensitive to input parameters.

**Index Terms**—Active Information Storage, Cellular Automata, Density Classification Task, GKL rule, Information, Mutual Information, Transfer Entropy

## I. INTRODUCTION

This paper has the dual goals of (1) using information-theoretic measures to better understand the computational dynamics of cellular automata (CAs), and (2) using such CAs as a vehicle to better understand the information-theoretic measures of entropy, mutual information, and transfer entropy. Along the way, we replicate some results from a previous project [1], and partially replicate and extend some results from Mitchell & colleagues [9] [11] and Lizier & colleagues [7] [13], relying heavily on Lizier's Java Information Dynamics Toolkit (JIDT) [4].

Mitchell & colleagues [11] [10] explored the computational dynamics of CAs, and the evolution of CA rule sets to solve a density classification task, eventually incorporating the computational dynamics framework of Crutchfield & Hanson [3] [2] to characterize the performance of their CAs. As Mitchell later remarked, “the language of particles and their interactions form an explanatory vocabulary for decentralized computation,” and provided insight (not available at the level of a CA-rule bit string) into the computational process of a CA [9].

In addition to the macro-level interpretation offered by a computational dynamic approach, one can also apply a variety of information-theoretic measures to CAs, possibly leading to further insights into CA computation, and at least

confirming or substantiating the macro-level interpretations in terms of particles and particle interactions. Such application can also benefit our understanding of the information measures themselves — e.g., what might be some practical, real-world manifestations and interpretations of abstract information-theoretic concepts such as entropy, mutual information, or local active information storage?

Before looking at methods and results, we briefly review some of the information-theoretic measures used later in the paper.

**Entropy ( $H$ )**. The *Shannon information content* or *local entropy* of an outcome  $x$  of measurement of the variable  $X$  is [4]:

$$h(x) = -\log_2 p(x) \quad (1)$$

and the *Shannon entropy* of a process or output  $X$ , representing the expected or average uncertainty associated with any measurement  $x$  of  $X$ , is:

$$H(X) = -\sum p(x) \log_2 p(x) \quad (2)$$

where the summation is over all possible output categories or alphabet symbols. For example, the local entropy of a single flip of a fair coin showing up heads is

$$\begin{aligned} h(\text{HEADS}) &= -\log_2 p(\text{HEADS}) \\ &= -\log_2 \left(\frac{1}{2}\right) \\ &= -(-1) = 1 \text{ bit} \end{aligned}$$

And such entropy is additive for independent events: the entropy of a 4-flip sequence such as HHTH is 4 bits, which gives an average of 1 bit per symbol.

Unfortunately, we often encounter such sequences of events without having external or *a priori* knowledge about the probabilities of the categories of sub-events making up the sequence — for example, suppose we witnessed the HHTH sequence of coin flips without knowing whether or not the coin is fair? In such a case, our best estimate of the probabilities associated with each toss outcome (HEADS vs. TAILS) comes from the sequence itself: it appears that HEADS has a probability of approximately  $\frac{3}{4}$  and TAILS a probability of approximately

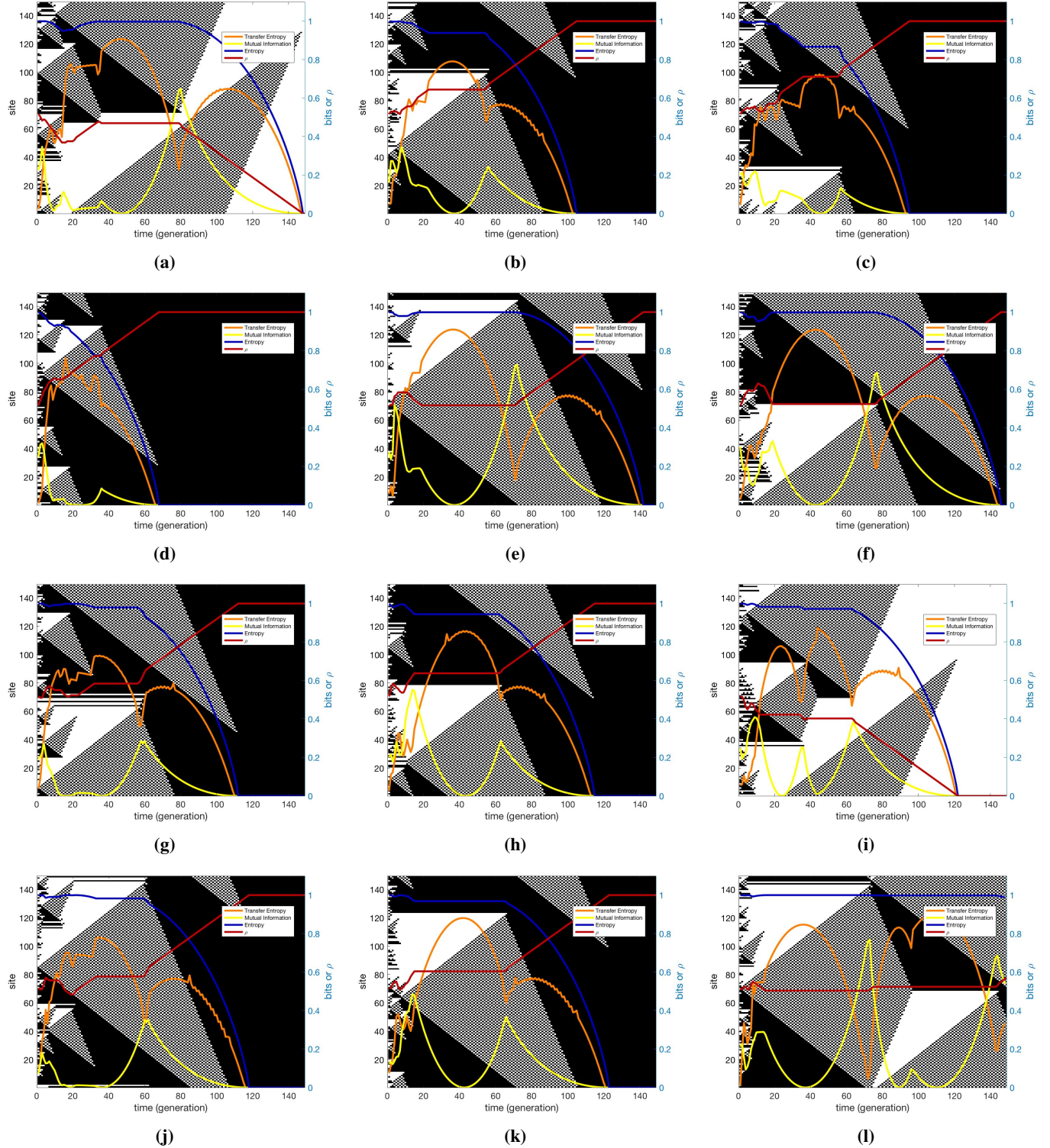


**Fig. 1:** Entropy (H), Transfer Entropy (TE), and Mutual Information (MI) (in terms of the average number of bits per cell) overlaid on the space-time diagrams for a sample of GKL-rule-based 149-cell cellular automata (CA). The CAs are shown evolving from left to right (instead of the more traditional top to bottom), producing generational (time-step) columns instead of rows. H of each column appears in dark blue. TE for columns  $x_i \rightarrow x_{i+1}$  is shown in orange. MI between columns  $x_i$  and  $x_{i+1}$  is shown in yellow.  $\rho$  (the proportion of 1s or black cells) is shown in red.  $\rho_0 = 0.52$  each time, and thus CAs ending with an all-black column (b–h, j, k) all represent correct density classification by the CA. CAs ending in an all-white column represent a mis-classification (a, i). Image (l) represents a classification failure where the CA failed to converge by the maximum time steps (but was clearly heading toward a mis-classification).

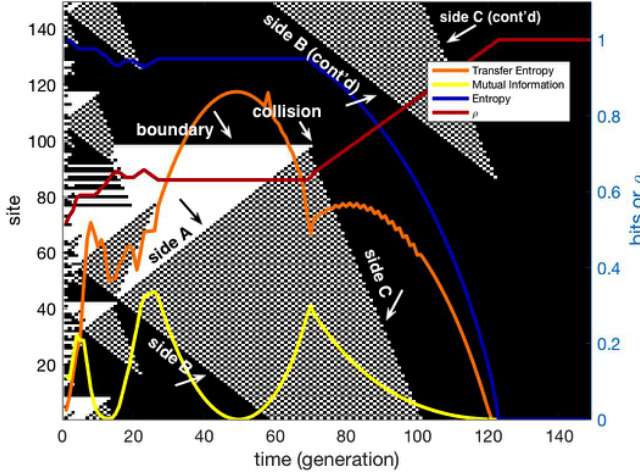


**Fig. 2:** The space-time diagram for a GKL-rule CA, with information-theoretic measures as in Fig. 1, and now labeled with important features (after [10] & [9]). In terms of the computational mechanics framework of Crutchfield & Hanson [3] [2], the white, black, and checkerboard regions correspond to “regular domains” (here corresponding respectively to regular languages  $0^*$ ,  $1^*$ ,  $(01)^*$ ). Sides A, B, and C are localized boundaries between domains and can be conceptualized as particles serving as information carriers, and a collision is a locus of information processing, where particles interact.

$\frac{1}{4}$ . (The longer the sequence of flips, of course, the more reliable our sequence-based estimate should be of the category probabilities.) In this case, the calculation of  $H(X)$ , then, for the HHTH sequence would be:

$$\begin{aligned} H(\text{HHTH}) &= -p(\text{H}) \log_2 p(\text{H}) - p(\text{T}) \log_2 p(\text{T}) \\ &= -\frac{3}{4} \log_2 \left(\frac{3}{4}\right) - \frac{1}{4} \log_2 \left(\frac{1}{4}\right) \\ &\approx 0.811 \text{ bit/symbol} \end{aligned}$$

In other words, we are now averaging *less* than 1 bit per symbol, because HEADS is more likely than TAILS. Note also that the entropy would be exactly the same for any one of the 3-head, 1-tail sequences THHH, HTHH, HHTH, HHHT. One can see why such entropy measures are often described as measuring unpredictability or disorder. This is the sense in which entropy will be measured below in each generation of the cellular automata, utilizing the sample itself to estimate the underlying probabilities.

**Mutual Information (MI).** As described in [5], the mutual information (MI) between  $X$  and  $Y$  measures the average reduction in uncertainty about  $x$  that results from learning the value of  $y$ , or vice versa:

$$\begin{aligned} MI(X; Y) &= - \sum_{x,y} p(x, y) \log_2 \frac{p(x|y)}{p(x)} \\ &= - \sum_{x,y} p(x, y) \log_2 \frac{p(x, y)}{p(x)p(y)} \\ &= H(X) - H(X|Y) \end{aligned} \quad (3)$$

As described in [14], “mutual information measures the information that  $X$  and  $Y$  share: It measures how much knowing one of these variables reduces uncertainty about the other.” MI is similar to correlation measures such as Pearson’s  $r$ , but MI is more general and captures information about non-linear dependence as well. For discrete values, the result is similar to  $\chi^2$ .

**Transfer Entropy (TE).** First developed by [12], transfer entropy can be described as “a non-parametric statistic measuring the amount of directed (time-asymmetric) transfer of information between two random processes. Transfer entropy from a process  $X$  to another process  $Y$  is the amount of uncertainty reduced in future values of  $Y$  by knowing the past values of  $X$  given past values of  $Y$ .” The formal definition looks like this:

$$T_{X \rightarrow Y}^{(k)} = - \sum_{x,y} p(y_{n+1}, x_n^{(k)}, y_n^{(k)}) \log \left[ \frac{p(y_{n+1}|x_n^{(k)}, y_n^{(k)})}{p(y_{n+1}|y_n^{(k)})} \right] \quad (4)$$

which also turns out to be equivalent to the following [15]:

$$\begin{aligned} T_{X \rightarrow Y}^{(k)} &= H(Y_t | Y_{t-1:t-L}) - H(Y_t | Y_{t-1:t-L}, X_{t-1:t-L}) \\ &= MI(Y_t; X_{t-1:t-L} | Y_{t-1:t-L}) \end{aligned} \quad (5)$$

meaning that TE is a form of conditional mutual information. Transfer entropy, both in its general *average* form above and in its localized version, can potentially detect where/when a computational process is effectively transferring information from one place or process to another.

**Local Active Information Storage (LAIS).** First developed and presented in [7], local active information storage is “a measure of the amount of information storage in use by the process at a particular time-step  $n + 1$ . It is the local mutual information (or pointwise mutual information) between the semi-infinite past of the process and its next state.” LAIS has a complex technical definition, related to what Lizier & colleagues term “excess entropy”, and they have championed its use in the analysis of CA behavior and in the dynamics of neural signals [7] [13]. We use the LAIS measure below in a preliminary effort to better understand its meaning and potential applications.

## II. METHOD & RESULTS

### A. Information-Theoretic Measures Applied to Gacs-Kurdyumov-Levin (GKL) binary-state Cellular Automata Performing a Density Classification Task.

We begin with some replication and mild extension of previous results involving CAs applying the so-called GKL rule to perform a density classification task (described and discussed in detail elsewhere [1] [11]). Info-theoretic measures were applied to a large sample of such CAs, and the results compared in the search for broad commonalities that might inform us about analogous commonalities in the underlying computational dynamics.

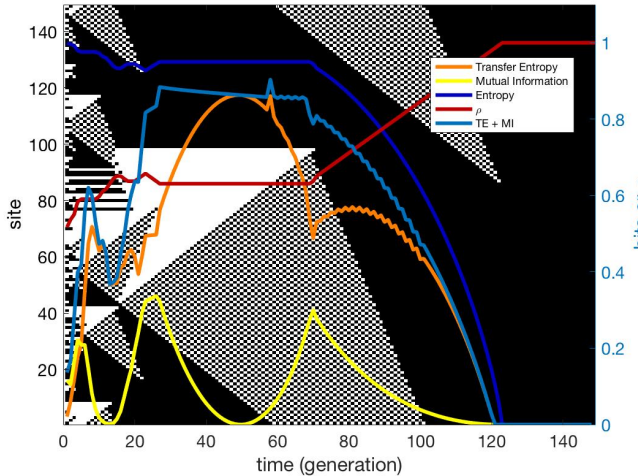


**Fig. 3:** The space-time diagram for a GKL-rule CA, like those in Fig. 1, but now also showing the TE + MI sum (light blue). Over a wide swath of the space-time diagram, H appears to differ by a constant amount from the sum TE + MI.

**METHOD.** MATLAB [8] was used to replicate and extend the analysis of some of the experimental results in [11] for the Gacs-Kurdyumov-Levin (GKL) binary-state CA (hereafter referred to more simply as the GKL rule or GKL-rule-based CA) applied to  $T_{1/2}$ , the  $\rho_c = 1/2$  density classification task. This extension into information-theoretic measures follows and replicates some of the work by Lizier & colleagues [7] [13].

The GKL rule was applied to one-dimensional CAs with lattice widths of  $N = 149$  and initial random configurations using  $\rho_0 = 0.52$  (*i.e.* the proportion of 1s was approximately 0.52). Previous work [1] [11] suggests that results from a lattice width of  $N = 149$  are overall very similar to results obtained using larger lattices. For this work, a single  $\rho_0$  also served well — instead of looking at CA performance over a wide range of  $\rho_0$  values, we are instead more interested in the computational dynamics for CAs that solve (or don't solve) the classification task.  $\rho_0$  values close to  $1/2$  produce CA arrays with more extended periods of computational dynamics, but don't produce qualitatively different dynamics compared to  $\rho_0$  values closer to the extremes of 0 or 1.

Letting the  $i$ th generation or time-step of the CA be considered a vector  $x_i \in \{0, 1\}^{149}$ , the following information-theoretic measures were then applied to the resulting CA lattices, using Lizier's Java Information Dynamics Toolkit [4]

- entropy (H) of each  $x_i$  (in average number of bits per cell);
- transfer entropy (TE) from each  $x_i$  to  $x_{i+1}$  (in average number of bits per cell);
- mutual information (MI) between each pair  $x_i$  to  $x_{i+1}$  (in average number of bits per cell);
- the *local* transfer entropy (LTE, in bits) for each cell in

the lattice;

- and the *local* active information storage (LAIS, in bits) for each cell in the lattice.

Each CA computational process was allowed to run for  $m = 149$  generations.

**RESULTS.** The H, TE, and MI measures are shown for a diverse but typical sample of CAs in Fig. 1. The CAs are shown evolving from left to right (instead of the more common top to bottom), with the information measures overlaid on each array and scaled using the right-hand vertical axis (in *bits* for information measures and as a proportion 0–1 for  $\rho$ ). It's important to realize that the information measures here are actually *average* measures, expressed as the average number of bits per symbol or bits per cell.

**$\rho$  Values.**  $\rho$  measures the proportion of 1s in each generation of a CA and is plotted in dark red in each space-time diagram.  $\rho$  is not an information-theoretic (IT) measure, but turns out to be very useful to explicitly consider when trying to understand the underlying computations being performed by the CA. (1) Notice first that  $\rho$  is generally not monotonic. One might very easily have thought that in correct-classification sequences, one would see a gradual but steady “relaxation” of the underlying cell values to all 1s, but the reality is more complicated, with  $\rho$  often having a local maximum and retreating to a lower but relatively constant value for many generations before continuing back on its track toward  $\rho = 1$ . (2) Typical of both correct classifications and mis-classifications is a middle-generation period of relatively constant  $\rho$  values (see generations 20–60 in Fig. 1(e), for example), which seems to correspond to the decision-making process associated with the beginning-to-middle phase of the final checkerboard-pattern evolution. (3) This is then routinely followed by a linear change in  $\rho$  values to the relaxed  $\rho = 1$  or  $\rho = 0$  value, starting at the final barrier/particle collision-interaction (see below for further discussion of computational mechanics framework). And (4) the  $\rho$  function pattern is a reliable early-indicator for the likely success or failure of the classification. An early drop in  $\rho$  generally leads to a misclassification, and such early-warning signs seem to set in within the first 10 generations or so.

In this and further discussion below, it is useful and important to eventually relate the information-theoretic measures to the computational mechanics framework of Crutchfield & Hanson [3] [2]. A typical space-time diagram for a GKL-rule CA is shown in Fig. 2, including the same set of information-theoretic measures being discussed, but now also including labels for important dynamical structural features. The white, black, and checkerboard regions correspond to “regular domains.” The sides of the triangular checkerboard regions are localized boundaries between domains and can be conceived as carriers of information in the form of particles traveling across the space-time diagram. Abutting white-black regions form boundaries, which then interact (in the form of collisions) with the information-carrying particles from other

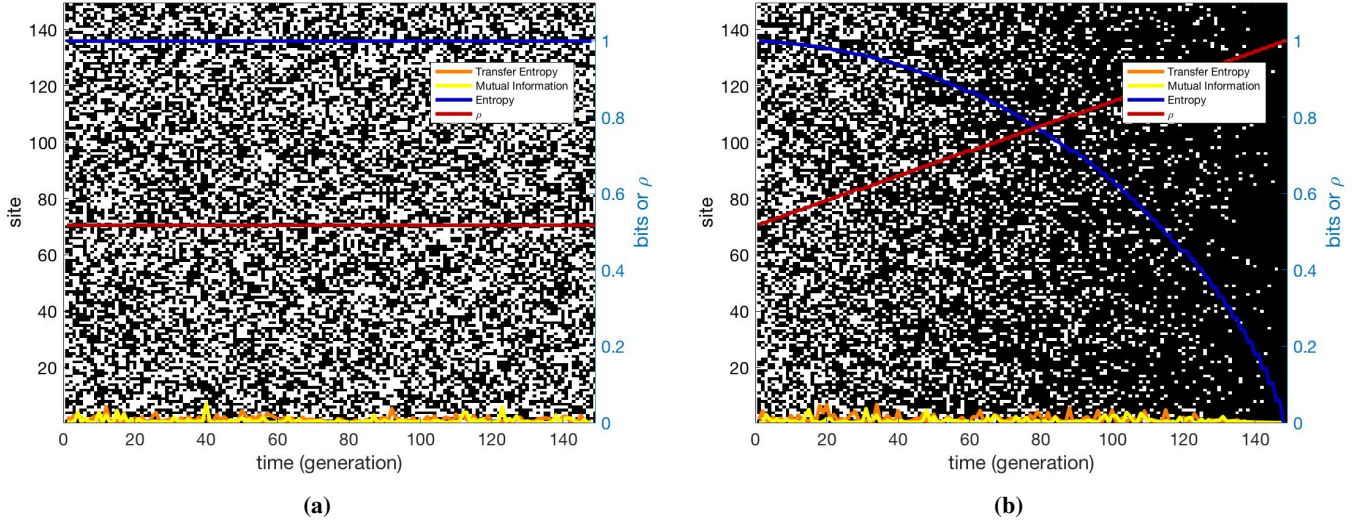


**Fig. 4:** Entropy (H), Transfer Entropy (TE), and Mutual Information (MI) analysis results for pseudo-cellular automata in which each generation was created randomly to match a desired proportion of 1s or black cells ( $\rho$  in the work, for example, of [11]). In (a): each generation had  $\rho \approx 0.52$ , to directly compare to the analyses shown in Fig. 1 above. In (b): the initial generation had  $\rho \approx 0.52$  and  $\rho$  decreased at a constant rate to end at  $\rho = 0$  in the last generation. As in Fig. 1, these pseudo-CA were 149 cells wide (tall in the figure) and are shown “evolving” from left to right for 149 generations.

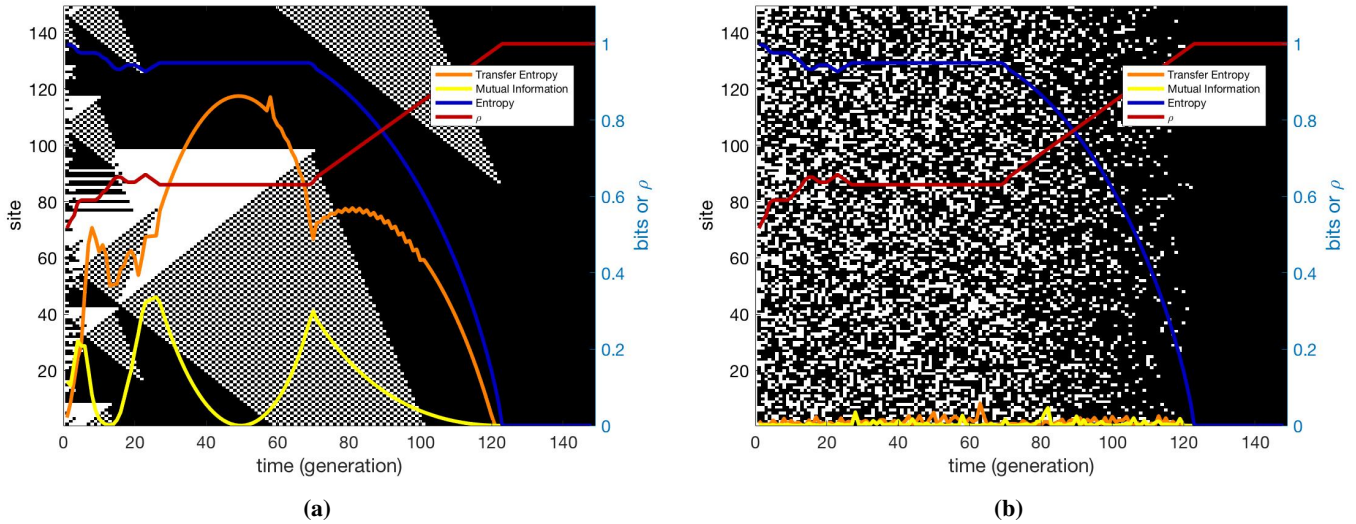


**Fig. 5:** Entropy (H), Transfer Entropy (TE), and Mutual Information (MI) analysis results for a cellular automaton (CA) vs. a  $\rho$ -matched pseudo-CA. (a) A 149-cell CA with GKL rule and  $\rho_0 \approx 0.51$  (shown evolving from left to right). (b) The corresponding pseudo-CA, using randomized 0s and 1s in which the  $\rho$  values for each generation (red line) match the  $\rho$  values for the standard CA in (a). TE and MI are essentially zero throughout all generations of the pseudo-CA, confirming that TE and MI for the standard CA reflect important structural dynamics instead of artifacts related to large-scale systematic distribution of density values.

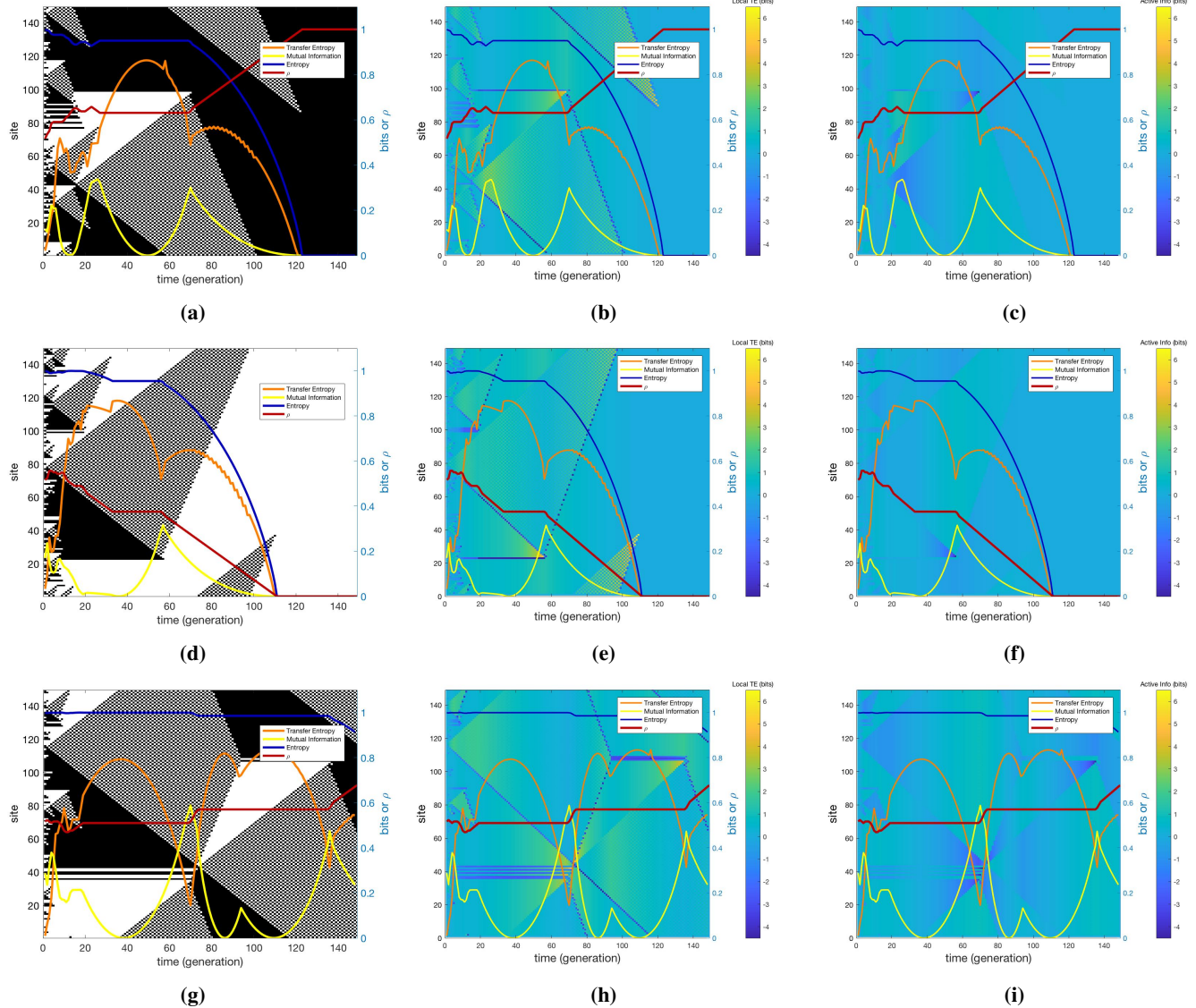


**Fig. 6:** Local transfer entropy (LTE) and local active information storage (LAIS) measures for a sample of cellular automata (CAs). **Each row:** first shows the space-time diagram for a CA, then its corresponding color-mapped representations of LTE and LAIS. The first row uses the same GKL-rule CA from Figs. 2, 3, & 5(a). Across a wide variety of CA space-time dynamics, we see high LTE at the beginning and resolution of the regular checkerboard domains, and a peak in LTE associated with collisions. For the first two CAs, LTE and LAIS values are essentially 0 for all cells starting around generation 128.

areas of the space-time domain.

**Entropy values.** The entropy values are linked to the  $\rho$  values, and the results both confirm this and allow us to understand the relationship. Recall the introductory comments above about entropy measures:  $H$  is being measured by using each generation's extant 0 and 1 distribution to estimate the probabilities  $p(0)$  and  $p(1)$  for the  $H$  calculation.  $p(1)$ , though, is actually the generation's value for  $\rho$ .  $H$  begins in each CA at approximately 1. With  $\rho \approx 0.52$ , we have  $p(1) \approx p(0) \approx \frac{1}{2}$  and thus entropy should be approximately 1 bit per symbol. For CAs that eventually classify (whether correct or incorrect),  $H$  is eventually 0, because the final CA string consists of all 0s or all 1s. In between we see two broad phases: a roughly

constant phase with  $H \approx 1$ , as the CA processes the input but doesn't end up changing the  $\rho$  values very much, then a parabolic drop in  $H$  (roughly a function of  $\rho^2 \log \rho$ ), beginning with the final particle-barrier collision (see around generation 70 in Fig. 1(e) for an example). Interestingly, that final particle-barrier collision is also the generation in which we see striking mirror pairs of local extrema in the transfer entropy and mutual information, which we discuss next below.

**Transfer Entropy and Mutual Information.** TE and MI exhibit an imperfect but striking inverse relationship throughout most of these space-time diagrams, bounded above by the entropy. (1) This roughly inverse relationship can be understood at the conceptual level as a reflection of the fact that high MI indi-

cates high shared information rather than information transfer, and high TE indicates high information transfer which should manifest as lower mutual information. More technically, recall that TE can be expressed as a form of conditional mutual information. We should (eventually) be able to formulate the mathematical relationship among H, TE, and MI. This relationship is further hinted at in Fig. 3, which shows the collection of information-theoretic measures for another CA, and this time also plots the sum TE + MI (shown in light blue). Over a large extent of the space-time diagram, the entropy and the TE + MI sum appear to differ by a constant amount. (2) As mentioned earlier in the discussion of entropy, we see very reliable, highly distinctive local extrema (a local max for MI and a local min for TE, both in the form of cusps) coinciding with the final particle-barrier collision in the space-time diagrams. Such mirrored cusps manifest multiple times in some space-time diagrams, where the computational dynamics proved more complex or extensive and provided more numerous large-scale particle-barrier interactions (see, for example, Fig. 1(h, i, l)). The significance of these distinctive and rather dramatic patterns is still unclear, but appear important and promising for future deeper understanding of the underlying computational dynamics.

A few follow-up observations are in order before proceeding to consider the local transfer entropy (LTE) and local active information storage (LAIS) measures. One might be concerned that the distinctive patterns of H, TE, and MI are simply artifacts of some underlying noisy process in the distribution of cell values and have little to do with actual computational dynamics per se. To alleviate this concern, we can look at the same information-theoretic measures applied to a “pseudo-cellular automaton” in which the deterministic computational rule has been removed and the generation-to-generation transformations are instead determined by simple functions of the density value  $\rho$ . Examples of these comparison conditions appear in Figs. 4 and 5.

Fig. 4 shows the information-theoretic measures discussed so far applied to (a) a pseudo-CA in which the density of 1s in each generation is simply kept constant at  $\rho = 0.52$ , and (b) a pseudo-CA in which the density of 1s changes linearly from  $\rho = 0.52$  to  $\rho = 1$ . In both cases, we see the expected function for entropy (one constant, the other dropping from 1 to 0), but with essentially zero values for the TE and MI measures. Fig 5 makes this point even more clearly, showing side-by-side a standard space-time diagram for a CA and a pseudo-CA matched generation-by-generation to the real CA in terms of  $\rho$  values. The highly distinctive structure of the TE and MI measures collapses without the underlying computational dynamics, despite the matching  $\rho$  values in the developmental trajectory.

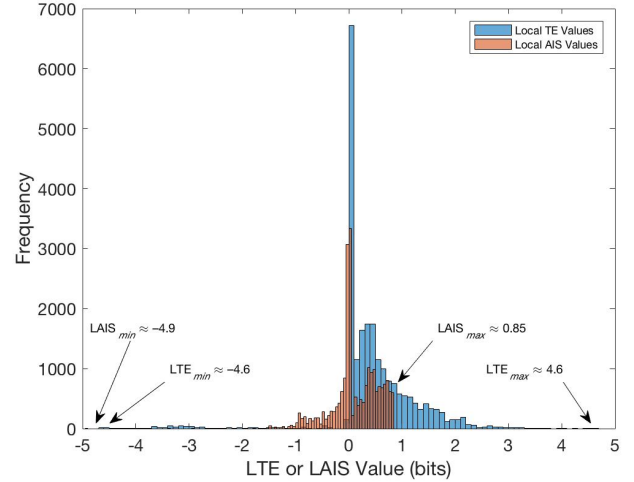


**Fig. 7:** Distribution of local transfer entropy (LTE) and local active information storage (LAIS) values for example CA of Fig. 6(a). LTE values ranged approximately from  $-4.6$  to  $4.6$  with a mean of  $0.46$  bits; LAIS values ranged approximately from  $-4.9$  to  $0.85$  with a mean of  $0.18$  bits.

### B. Local Transfer Entropy (LTE) & Local Active Information Storage (LAIS) in the Computational Dynamics of GKL-rule-based Cellular Automata

In addition to the distributed or average information-theoretic measures explored earlier, we now look at at localized measures of transfer entropy (LTE) and active information storage (LAIS) in the computational dynamics of the same class of GKL-CA in the process of solving the  $\rho_c = 1/2$  density classification task.

These local measures are intriguing: They could help identify particular regions of space-time developmental trajectories in which interesting computational processes are occurring. Moreover, unlike the distributed IT measures, which are always non-negative, these localized measures can take on negative values, and can take on absolute values larger than the intuitively expected limit of  $\log_2(|\Sigma|)$ . For example, with an alphabet  $\Sigma = 0, 1$  for our binary strings, one would expect local information measures to be limited to at most 1 bit/cell. These local IT measures, however, take into account local use or transfer of information across temporal and spatial extents, and acknowledge that information in use or being transferred at a location may be stored in nearby cells. The localized information being used or transferred, then, might be well above the information limit for that particular cell or location considered in isolation. Lizier & colleagues [7] describe LAIS, for example, as “a measure of the amount of information storage in use by the process at a particular time-step .... It is the local mutual information (or pointwise mutual information) between the semi-infinite past of the process and its next state.” In other words, LAIS explicitly measures “how much of the information from the past of the process is observed to be in

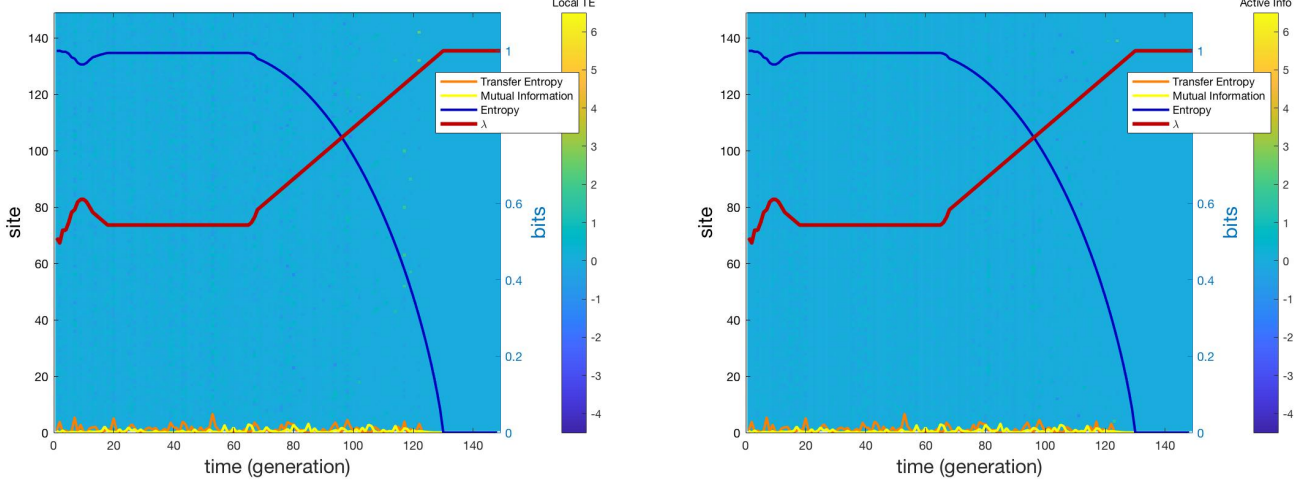


**Fig. 8:** Local transfer entropy (LTE) and local active information storage (LAIS) measures for a pseudo-CA  $\rho$ -matched to the space-time CA diagram of Fig. 6(a). LTE and LAIS is essentially 0 throughout the space-time diagram for the pseudo-CA, further confirming that the distinctive patterns of LTE and LAIS seen in Fig. 6 is due to the underlying computational dynamics of the CA.

use in computing its next state” [6].

**METHOD.** The general method was almost identical to that previously described, using MATLAB [8] to generate GKL-rule-based CAs, and in conjunction with Lizier’s JIDT [4], apply information-theoretic measures to the space-time trajectories of the CA. Now, in addition to the distributed measures of H, TE, and MI, the local measures LTE and LAIS were included, and MATLAB was used to color-map the resulting local measures onto the space-time diagrams.

**RESULTS.** The main results for these local information-theoretic measures are shown in Figs. 6, 7, & 8. Fig. 6 shows the typical results, sampled from hundreds of such runs, for three categories of CAs: a correct density classification result (row 1), a mis-classification (row 2), and an incomplete classification (row 3). Each row shows the original space-time diagram for the CA (as before, evolving from left to right), then color-mapped images of the LTE and LAIS. The first row uses the same CA that appears in Figs. 2, 3, and 5(a), to allow ease of comparisons.

In the discussion below, it is useful to refer to particular locations in the space-time diagrams. For this purpose we simply use approximate  $x,y$ -coordinates in the usual way, and omit the “approximate” notation each time when doing so.

**Local Transfer Entropy (LTE).** Across a wide sampling of GKL-rule space-time dynamics, we see high levels of LTE at the beginning and conclusion of the regular checkerboard domains (see, for example, locations (25, 45) and (120, 90) in Fig. 6(b)). We also see peaks in LTE at collisions, such as seen at location (67, 97) in Fig. 6(b). This is somewhat gratifying, apparently corroborating the computational mechanics framework interpretation of collisions as a location of information processing and transformation; this also seems consistent with our understanding of the checkerboard regions as manifesta-

tions of a computational process sharing information across the space-time diagram about local relative densities. Throughout the checkerboard regions we see largely non-negative LTE values, indicating a diffuse information transfer process, that is then “concentrated” as the checkerboard pattern eventually resolves, signaling a final decision.

More puzzling is the LTE associated with gliders or particles, such as we see for regional barriers (appearing as horizontal gliders in our diagrams) and particles at the edges of the checkerboard domains (appearing as the extended sides of the triangular checkerboard domains). Such barriers and particle paths are consistently marked with substantially negative LTE values. This is consistent with some results from Lizier & colleagues [6]. They point out that “Negative values imply that the source misinforms an observer about the next state of the destination in the context of the destinations past,” and that we will often see negative values for gliders moving obliquely with respect to the main time axis. This makes some intuitive sense — perhaps the LTE computations would need to be hand-tuned to incorporate some spatial-temporal phase shift to allow it to capture the local TE manifesting in the obliquely-appearing dynamical patterns. More problematic for our results, though, is the apparent negative LTE values associated with our horizontal gliders (corresponding to a white-to-black “barrier” such as that appearing in locations (20-75, 98) in Fig. 6(b)). This consistent result seems to conflict with expectations for LTE and appears to contradict typical results reported by Lizier & colleagues under similar conditions [7] [5]. There are clearly complications here in naively applying the LTE measure, and future work should examine more carefully the LTE calculation parameter options.

**Local Active Information Storage (LAIS).** Across a wide sampling of GKL-rule CA space-time dynamics, we see mild levels of positive LAIS distributed throughout the lattice,

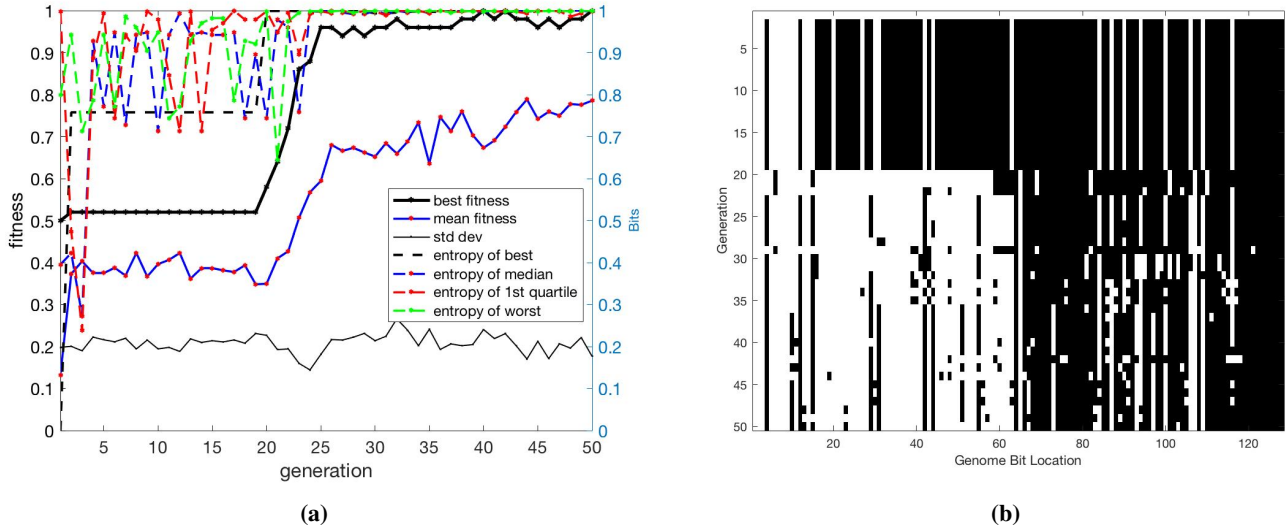


**Fig. 9:** Some inspiration for future work, looking at the relationship between CA rule fitness and rule entropy for CA rules developed using genetic algorithms. (a) Fitness and entropy values for CA rules evolved using a genetic algorithm to solve the density classification problem. Entropy values are shown for best-fit, median-fit, worst-fit, and 1st-quartile-fitness in each generation. (b) Color-map plot of the evolved best-fit CA rules, showing the qualitative shift in internal bit-wise organization around generation 20 in this particular evolutionary run.

along with considerable levels of negative LAIS values. This again presents a complicated and nuanced picture of what LAIS actually seems to mean and what it tells us about the computational dynamics.

Consistent with the definition and interpretation of LAIS, we see mild positive levels of LAIS accrue over time within the checkerboard regions; this suggests the accumulation of the decision-making information over space-time as the checkerboard region boundaries share information across space and eventually “decide” on the density classification. Interestingly, we also see negative LAIS values concentrated in the neighborhoods of collisions. Lizier & colleagues explain this in part due to the information-carrying particles traveling through those regions which then modify the information-carrying properties of local cells. Another possibility is that the LAIS becomes increasingly negative as the collision approaches, because such a collision indicates an imminent change in the density classification in that region (going from white to black, for example).

To give a better sense of the underlying distribution of LTE and LAIS values documented in these CAs, the distributions of LTE and LAIS values are shown in Fig. 7 for the CA shown in the first row of Fig. 6. Local measures close to 0 strongly dominate the distributions, and extreme negative values are actually quite rare in comparison. LTE values are largely non-negative and larger in value than the LAIS values, suggesting an underlying process dominated more by a systematic transfer of information rather than a process focused on storage of information. This makes some intuitive sense as well, with the eventual “relaxation” of the CA cells to all 0s or all 1s representing more a transformation of information than a preservation or storage of information.

As we did for the distributed IT measures earlier, it is also useful to carefully document the LTE and LAIS measures on  $\rho$ -matched pseudo-CAs. In Fig. 8, we see the LTE and LAIS measures for a pseudo-CA that has been exactly  $\rho$ -matched to the space-time, LTE, and LAIS diagrams of the CA that appears in the first row of Fig. 6. LTE and LAIS are both essentially 0 throughout the space-time diagram of such a matched pseudo-CA. This confirms that the distinctive patterns of LTE and LAIS seen in computationally “real” CAs such as seen in Fig. 6 are due to the underlying computation dynamics and are not just artifacts of the changing arrangements of cell values nor a misapplication of the measurement tools.

### III. DISCUSSION & CONCLUSIONS.

In this paper we briefly reviewed some commonly (or increasingly commonly) used information-theoretic measures, and explored the application of those measures to some standard GKL-rule-based cellular automata to better understand the computational dynamics of the CAs and to better understand the IT measures themselves. Along the way, we have replicated some previous results [1] [11] [6], extended some of those results to include IT measures, and discovered some puzzling results in apparent conflict with earlier results.

The results enable a better understanding of entropy: how it manifests in CA-based computational dynamics and what it might mean about the underlying computations. We saw, for example, the CA dynamics largely preserve entropy until a critical point at which the process seems to commit to an underlying computational decision, at which time the entropy quickly drops. The results also suggest some surprising interrelationships among H, TE, and MI, which future work can better elucidate. For large swaths of the space-time region of

CA performance (but notably *not* for the entire computation), H and the sum TE + MI appear to differ by a constant value. The results also document the potential for local IT measures such as LTE and LAIS to inform about the underlying computational dynamics, but simultaneously verify the difficulty of interpretation of such local IT measures, especially the meaning of negative values. In retrospect it becomes more clear just why so much of the content of Lizier & colleagues' work involves the intricate exploration and elaboration of the fine-tuning of parameters needed to usefully capture the most (and most relevant) LTE and LAIS.

This work is obviously preliminary, and would benefit from future exploration of a wider variety of cellular automata under a wider variety of conditions; our understanding and interpretation would also benefit from applications of IT measures to the evolution of CA rules using genetic algorithms. For example, the application of simple entropy measures to the CA rules obtained from a genetic algorithm for evolving GKL-like rules to solve the density classification problem gives us insight into the underlying evolutionary process and population of evolved rules — see Fig. 9 below. It will be interesting to look at TE, MI, and local versions of IT measures applied to such rule populations evolving to solve particular problems.

#### IV. AUTHOR CONTRIBUTIONS

The author worked by himself on this project, but also used (and further developed) MATLAB code used in a previous project (and that earlier code was developed by the author himself as well).

#### REFERENCES

- [1] A. Anderson and W. D. Craft. Observations on the evolution of cellular automata using genetic algorithms. 2018. A report for Computer Science 523, Complex Adaptive Systems, University of New Mexico, 2018.
- [2] J. P. Crutchfield and J. E. Hanson. Turbulent pattern bases for cellular automata. *Physica D: Nonlinear Phenomena*, 69(3-4):279–301, 1993. Retrieved from <https://pdfs.semanticscholar.org/3ed7/3adcc1faaa76800afcfc233b2edd2560ca0b7.pdf>.
- [3] J. E. Hanson and J. P. Crutchfield. The attractorbasin portrait of a cellular automaton. *Journal of Statistical Physics*, 66(5/6):1415–1462, 1992. Retrieved from <https://pdfs.semanticscholar.org/d3a1/3530684e39f97272b569b6968a39554c627c.pdf>.
- [4] J. T. Lizier. Jidt: An information-theoretic toolkit for studying the dynamics of complex systems. *Frontiers in Robotics and AI*, 1(11), 2014. doi: 10.3389/frobt.2014.00011.
- [5] J. T. Lizier. Measuring the dynamics of information processing on a local scale in time and space. In M. Wibral, R. Vicente, and J. Lizier, editors, *Directed Information Measures in Neuroscience: Understanding Complex Systems*, pages 161–193. Springer, Berlin, Heidelberg, 2014.
- [6] J. T. Lizier and J. R. Mahoney. Moving frames of reference, relativity and invariance in transfer entropy and information dynamics. *Entropy*, 15:177–197, 2013. doi:10.3390/e15010177.
- [7] J. T. Lizier, M. Prokopenko, and A. Y. Zomaya. Local measures of information storage in complex distributed computation. *Information Science*, 208:39–54, 2012. doi: 10.3389/frobt.2014.00011.
- [8] MATLAB. version 9.2.0 (R2017a). The MathWorks Inc., Natick, Massachusetts, 2017.
- [9] M. Mitchell. *Complexity: A Guided Tour*. Oxford University Press, New York, NY, 1st edition, 2009.
- [10] M. Mitchell, J. P. Crutchfield, and R. Das. Evolving cellular automata with genetic algorithms: A review of recent work. *Proceedings of the First International Conference on Evolutionary Computation and Its Applications*, 1996. Retrieved 5/6/2018 at <http://csc.ucdavis.edu/evca/Papers/evca-review.pdf>.
- [11] M. Mitchell, J. P. Crutchfield, and P. T. Hraber. Evolving cellular automata to perform computations: Mechanisms and impediments. *Physica D*, 75(1-3):361–391, 1994.
- [12] T. Schreiber. Measuring information transfer. *Physical Review Letters*, 85(2):461–464, 2000.
- [13] M. Wibral, J. T. Lizier, S. Vgler, V. Priesemann, and R. Galuske. Local active information storage as a tool to understand distributed neural information processing. *Frontiers in Neuroinformatics*, 8:1–11, 2014.
- [14] Wikipedia contributors. Mutual information — Wikipedia, the free encyclopedia, 2018. [Online; accessed 8-May-2018].
- [15] Wikipedia contributors. Transfer entropy — Wikipedia, the free encyclopedia, 2018. [Online; accessed 9-May-2018].